The Performance Analysis of Thermal Effect in Mesh-Based Optical Networks-on-Chips

Junxiong Chai, Lixia Fu, Yiyuan Xie, *Member, IEEE*, Tingting Song, Yichen Ye, Bocheng Liu, Li Dai, and Yong Liu, *Senior Member, IEEE*

***Abstract*—Optical networks-on-chips (ONoCs) are the key technology for the sustainable development of multiprocessors system-on-chip (MPSoC) in the future. Micro-ring resonators (MRs) are widely used in ONoCs as key device to select and redirect optical signals. However, MRs have the inherent property of being sensitive to environmental temperature. With the fluctuation of environmental temperature, its resonance wavelength drifts, which can introduce more loss and crosstalk noise to ONoCs and make the network performance decline sharply. Therefore, it is very important to analyze the influence of thermal effect in ONoCs to solve this problem. In this paper, the theoretical models of loss and crosstalk noise changing with temperature are established from device level to network level, respectively. And a series of network performances of mesh-based ONoCs caused by thermal effect are systematically modeled and analyzed employing formal methods. Finally, we conduct case studies for mesh-based ONoCs using optimized crossbar optical router and crux optical router to evaluate the proposed method. The simulation results show that the performance of mesh-based ONoCs declines with the increase of temperature, such as the decrease of optical signal-to-noise ratio (OSNR) and the increase of bit error rate (BER), which severely limits the network scalability. The formal analytical models provide a criterion for the performance analysis of thermal effect in ONoCs. In addition, the formal methods have high portability and scalability, and can provide technical support for future research work.**

***Index Terms*—Thermal effect, micro-ring resonators (MRs), optical networks-on-chips (ONoCs), optical crosstalk noise, optical losses.**

Manuscript received August 4, 2021; revised August 15, 2021; accepted August 17, 2021. Date of publication August 20, 2021; date of current version September 9, 2021. This work was supported in part by the Natural Science Foundation of Chongqing City under Grant cstc2016jcyjA0581, in part by the Postdoctoral Science Foundation of China under Grant 2016M590875, and in part by the Fundamental Research Funds for the Central Universities under Grant XDJK2018B012. *(Corresponding author: Yiyuan Xie.)*

Junxiong Chai, Lixia Fu, Tingting Song, Yichen Ye, Bocheng Liu, and Li Dai are with the College of Electronic and Information Engineering, Southwest University, Chongqing 400715, China (e-mail: 546194706@qq.com; 1103215934@qq.com; ttsong_53@163.com; ycye451@swu.edu.cn; 525795541@qq.com; 1535430544@qq.com).

Yiyuan Xie is with the Chongqing Key Laboratory of Nonlinear Circuits and Intelligent Information Processing, National Joint Engineering Laboratory of Intelligent Transmission and Control Technology, College of Electronic and Information Engineering, Southwest University, Chongqing 400715, China, and also with the School of Optoelectronic Information, University of Electronic Science and Technology of Chengdu, Sichuan 611731, China (e-mail: yyxie@swu.edu.cn).

Yong Liu is with the School of Optoelectronic Information, University of Electronic Science and Technology of Chengdu, Sichuan 611731, China (e-mail: yongliu@uestc.edu.cn).

Digital Object Identifier 10.1109/JPHOT.2021.3106318

I. Introduction

OPTICAL networks-on-chips (ONoCs) are the new kind of networks-on-chip for multi-processors system, which have the advantages of high bandwidth, low latency and low loss. And ONoCs can solve the parasitic effect of interconnects on chip caused by the increase of circuit integration and working frequency in traditional electrical interconnection network [1]. In ONoCs, silicon-based devices are widely used because of their characteristics of easy integration, low loss and low cost [2]. Among them, silicon-based micro-ring resonators (MRs), as essential device for optical signal selection and reorientation, play important role in the field of optical communication. Generally, MRs in ONoCs work in two states: resonant (ON) and non-resonant (OFF). Ideally, MRs in resonant and non-resonant states should maximize the coupling and passage of optical signal power.

However, thermal sensitivity is the inherent characteristic of MRs as photonic device, so their characteristics can be affected by temperature fluctuates. Previous studies have shown that chip temperature fluctuates in time and space, and under typical operating conditions, the steady-state temperature of the whole chip can vary more than 30 °C [3]. The temperature change seriously affects the characteristics of MRs, which leads to the shift of MRs resonance wavelength. When the resonance wavelength of MRs drifts, it causes the mismatch between the resonance wavelength and the working wavelength with valid information, thus introducing additional crosstalk noise and loss, resulting in the degradation of ONoCs performance. A large number of studies have shown that the accumulation of loss and crosstalk noise can affect integrity of information transmitted in the network and limit the scalability of network, greatly degrading the network performance of ONoCs [4]–[7]. With the change of temperature on chip, the additional loss and crosstalk noise caused by thermal effect are inevitably generate and increase, which further degrades the performance of ONoCs.

Recently, researchers have presented a series of studies for the thermal effects on ONoCs [8]–[10]. The results show that the thermo-optic effect of silicon photonic devices on ONoCs is mainly due to the thermal reaction of silicon. Silicon has obvious thermo-optic effect, and its effective refractive index increases linearly with temperature approximately. The change of MRs effective refractive index can directly affect their resonant wavelength [11], while the loss of optical switching elements in ONoCs composed of MRs has a corresponding relationship with resonant wavelength of MRs [12], [13]. The loss of switching

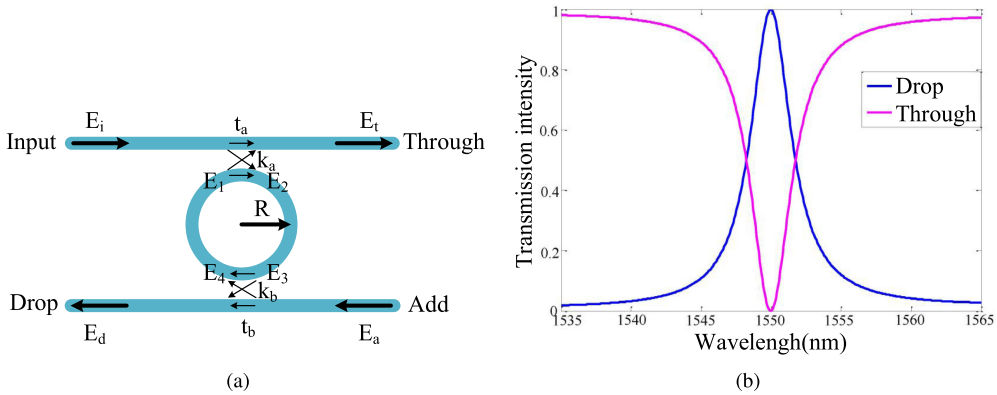

Fig. 1. (a) Basic structure of the Add-Drop micro-resonator. (b) Transmission spectra of Add-Drop micro-resonator in ON state at 30 °C.

elements caused by thermal effect is analyzed and discussed [14]. Moreover, many researchers have analyzed the impact of thermal variance and how to solve this problem [9], [15]–[17]. The most common solutions are to cool down the MRs or thermal tuning [18]. In order to propose a better solution, it is necessary to analyze the performance of ONoCs affected by thermal effect. However, there is still lack of a systematic and comprehensive analysis model for ONoCs performance problems caused by thermal effects.

In this paper, we start with the basic switching element level, analyze the loss and crosstalk noise caused by thermal effect accurately and systematically. Then we model and analyze the network performance of mesh-based ONoCs caused by thermal effect at routing level and network level. The main contributions are as follows: Firstly, based on the temperature dependence of the MRs, the theoretical models of power loss coefficient and crosstalk noise coefficient with temperature in optical switching element are given. Secondly, the formal analytical models of mesh-based ONoCs loss, crosstalk noise, optical signal-to-noise ratio (OSNR) and bit error rate (BER) caused by thermal effect are established. Finally, we evaluate the proposed models by numerical simulation of mesh-based ONoCs using different routers. In the numerical simulation process, we use different routers and calculate different optical links of mesh-based ONoCs, and finally find out the worst SNR link to evaluate the performance of ONoCs caused by thermal effect. The simulation results show that no matter which router is employed, the performance of mesh-based ONoCs will be affected by the temperature fluctuation, such as OSNR, BER, and network size, etc.

II. Characteristic Analysis of MRs Based on Thermal Effect

The basic photonic devices in ONoCs are switching elements, which are widely used in optical routers and networks. The MRs are an important part of the basic optical switching elements. Therefore, the characteristics of MRs have an important impact on the performance of ONoCs. Most of the MRs used in ONoCs are Add-Drop structure, as shown in Fig. 1(a). It consists of a ring waveguide and two straight waveguides, and two coupling regions are formed between them. The relationship between the optical fields of the straight waveguide and the ring waveguide in the coupling region can be expressed as follows:

$$\begin{bmatrix} E_t \\ E_2 \end{bmatrix} = \begin{bmatrix} t_a & jk_a \\ jk_a & t_a \end{bmatrix} \begin{bmatrix} E_i \\ E_1 \end{bmatrix} \tag{1}$$

$$\begin{bmatrix} E_d \\ E_4 \end{bmatrix} = \begin{bmatrix} t_b & jk_b \\ jk_b & t_b \end{bmatrix} \begin{bmatrix} E_a \\ E_3 \end{bmatrix} \tag{2}$$

where k_a and k_b represent the coupling coefficient in the coupling region, t_a and t_b represent the transmission coefficient in the coupling region. j is an imaginary unit, which indicates the phase change of $\frac{\pi}{2}$ introduced in the coupling process between waveguides. When lossless coupling occurs, k and t have the following relationship:

$$|k^2| + |t^2| = 1 \tag{3}$$

The phase change of an optical signal which satisfies the resonant condition in the ring waveguide for one circle is as follows:

$$\theta = \beta \cdot 2\pi R = 4\pi^2 n_{eff} \frac{R}{\lambda_{res}} \tag{4}$$

where R, n_{eff}, and λ_{res} are the radius, effective refractive index, and resonant wavelength of the MRs, respectively. β is the propagation constant. For the first coupling domain, the field E_i is set as the reference signal and three equations are established to solve the field of the other three ports.

$$E_t = t_a \cdot E_i + jk_a \cdot E_1 \tag{5}$$

$$E_2 = jk_a \cdot E_i + t_a \cdot E_1 \tag{6}$$

When there is no optical signal input at the Add port, the light field of E_1 is obtained by the transmission of the field of E_2 through the ring waveguide.

$$E_1 = E_2 \cdot \alpha \cdot t_b \cdot exp(j \cdot \theta) \tag{7}$$

where α is the loss coefficient of optical signal propagating in the ring waveguide. By combining Eq. (5), (6) and (7), the following

formulas can be obtained:

$$E_t = \frac{t_a - \alpha \cdot t_b \cdot exp(j \cdot \theta)}{1 - \alpha \cdot t_a \cdot t_b \cdot exp(j \cdot \theta)} \cdot E_i \tag{8}$$

$$E_2 = \frac{jk_a}{1 - \alpha \cdot t_a \cdot t_b \cdot exp(j \cdot \theta)} \cdot E_i \tag{9}$$

$$E_1 = \frac{jk_a \cdot \alpha \cdot t_b \cdot exp(j \cdot \theta)}{1 - \alpha \cdot t_a \cdot t_b \cdot exp(j \cdot \theta)} \cdot E_i \tag{10}$$

According to the E_2, the equations of E_3 and E_d can be obtained as follows:

$$E_3 = E_2 \cdot \alpha^{\frac{1}{2}} \cdot exp(j \cdot \frac{\theta}{2}) = \frac{jk_a \cdot \alpha^{\frac{1}{2}} \cdot exp(j \cdot \frac{\theta}{2})}{1 - \alpha \cdot t_a \cdot t_b \cdot exp(j \cdot \theta)} \cdot E_i \tag{11}$$

$$E_d = E_3 \cdot jk_b = \frac{-k_a \cdot k_b \cdot \alpha^{\frac{1}{2}} \cdot exp(j \cdot \frac{\theta}{2})}{1 - \alpha \cdot t_a \cdot t_b \cdot exp(j \cdot \theta)} \cdot E_i \tag{12}$$

So the output light fields of Through port and Drop port are:

$$E_{through} = E_t = \frac{t_a - \alpha \cdot t_b \cdot exp(j \cdot \theta)}{1 - \alpha \cdot t_a \cdot t_b \cdot exp(j \cdot \theta)} \cdot E_i \tag{13}$$

$$E_{drop} = E_d = E_3 \cdot jk_b = \frac{-k_a \cdot k_b \cdot \alpha^{\frac{1}{2}} \cdot exp(j \cdot \frac{\theta}{2})}{1 - \alpha \cdot t_a \cdot t_b \cdot exp(j \cdot \theta)} \cdot E_i \tag{14}$$

Their corresponding light field energy are:

$$I_{through} = E_t \cdot E_t^* = \frac{t_a^2 + \alpha^2 \cdot t_b^2 - 2\alpha \cdot t_a \cdot t_b \cdot cos(\theta)}{1 + \alpha^2 \cdot t_a^2 \cdot t_b^2 - 2\alpha \cdot t_a \cdot t_b \cdot cos(\theta)} \cdot I_i \tag{15}$$

$$I_{drop} = E_d \cdot E_d^* = \frac{k_a^2 \cdot k_b^2 \cdot \alpha}{1 + \alpha^2 \cdot t_a^2 \cdot t_b^2 - 2\alpha \cdot t_a \cdot t_b \cdot cos(\theta)} \cdot I_i \tag{16}$$

MRs can accurately couple the optical signals whose wavelength is consistent with its resonance wavelength λ_{res} and discard other signals, which is one of its main working principles in ONoCs. The resonance condition of MRs can be described as:

$$2\pi R n_{eff} = m\lambda_{res}, (m = 1, 2, 3 \cdots) \tag{17}$$

The resonant state is usually called ON state, while nonresonant state is called OFF state. From Eq. (17), it is known that there is a linear relationship between the resonance wavelength λ_{res} and the effective refractive index n_{eff}. Therefore, when the effective refractive index changes with temperature fluctuation, the resonant wavelength also changes with temperature fluctuation. The relationship between λ_{res} and temperature T can be obtained as:

$$\lambda_{res} = \lambda_{res_0} + \mu \cdot (T - T_0) \tag{18a}$$

$$\mu = \frac{\Delta_{neff}}{m} \cdot 2\pi \cdot R = \frac{\lambda_{res_0}}{n_{group}} \cdot \frac{d_{neff}}{d_T} \tag{18b}$$

where λ_{res_0} and T_0 are the initial resonance wavelength of MRs and initial temperature. $\frac{d_{neff}}{d_T}$ is the thermo-optic effects coefficient of the material, and the thermo-optic effects coefficient of silicon is about $(1.86 \pm 0.08) \times 10^{-4}/K$ [19], [20]. The n_{group} is about 4.63 at 1550 nm [14].

The transmission spectra of MRs with resonance wavelength 1550 nm at initial temperature of 30 °C are obtained by FDTD simulation environment as shown in the Fig. 1(b). The data of Fig. 1(b) are derived and fitted by the function fitting tool in MATLAB. The transmission spectral function expression of Drop port of MRs with resonance wavelength of 1550 nm in ON state is obtained as follows:

$$\begin{aligned} Tr = {} & a_1 \cdot exp\left(-\left(\frac{\lambda - b_1}{c_1}\right)^2\right) + a_2 \cdot exp\left(-\left(\frac{\lambda - b_2}{c_2}\right)^2\right) \\ & + a_3 \cdot exp\left(-\left(\frac{\lambda - b_3}{c_3}\right)^2\right) + a_4 \cdot exp\left(-\left(\frac{\lambda - b_4}{c_4}\right)^2\right) \\ & + a_5 \cdot exp\left(-\left(\frac{\lambda - b_5}{c_5}\right)^2\right) \end{aligned}$$

$$\begin{array}{lll} a_1 = 0.1786 & b_1 = 1550 & c_1 = 1.033 \\ a_2 = 0.4294 & b_2 = 1550 & c_2 = 1.807 \\ a_3 = 0.2715 & b_3 = 1550 & c_3 = 3.395 \\ a_4 = 0.09591 & b_4 = 1550 & c_4 = 7.261 \\ a_5 = 0.0267 & b_5 = 1568 & c_5 = 54.35 \end{array} \tag{19}$$

When the temperature fluctuates, the resonance wavelength of MRs varies with the temperature, and the Eq. (18) combined with Eq. (19) can be used to obtain an expression of the transmission spectrum as a function of temperature.

$$\begin{aligned} Tr_T = {} & a_1 \cdot exp\left(-\left(\frac{\lambda - \mu T + \mu T_0 - b_1}{c_1}\right)^2\right) \\ & + a_2 \cdot exp\left(-\left(\frac{\lambda - \mu T + \mu T_0 - b_2}{c_2}\right)^2\right) \\ & + a_3 \cdot exp\left(-\left(\frac{\lambda - \mu T + \mu T_0 - b_3}{c_3}\right)^2\right) \\ & + a_4 \cdot exp\left(-\left(\frac{\lambda - \mu T + \mu T_0 - b_4}{c_4}\right)^2\right) \\ & + a_5 \cdot exp\left(-\left(\frac{\lambda - \mu T + \mu T_0 - b_5}{c_5}\right)^2\right) \end{aligned} \tag{20}$$

As shown in Fig. 2, The MRs and their initial transmission spectra are shown as the blue solid line rings and spectral lines, the virtual MRs and their transmission spectra after wavelength drift due to thermal effect are indicated by blue dotted line rings and spectral lines, and the working wavelength with effective information is represented by yellow dashed lines. In ON state, at initial temperature, most of the optical signals are coupled by MRs and output from the Drop port (in Fig. 2, the thickness of yellow line is used to indicate the power of the coupled optical signal). As the temperature fluctuates, the transmission spectrum

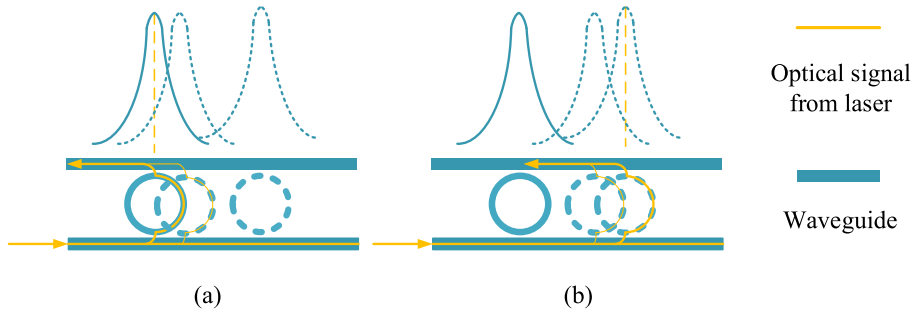

Fig. 2. Photonic transmission with thermal variations in MRs. (a) ON state. (b) OFF state.

of the MRs deviates, so that the transmittance of the working wavelength from laser decreases (the yellow dotted line that falls into the transmission line). In this case, only a small portion of the optical signal is coupled into the MRs, which results in more loss and crosstalk noise in ONoCs. In the case of large fluctuations in chip temperature, the thermal effect may even invalidate the MRs function, and most of the signals are directly output from the Through port. In the OFF state, almost all optical signals are output from the Through port at the initial temperature. With the change of temperature, when the resonance wavelength of MRs deviates near the working wavelength, a small amount of optical signals are coupled into MRs and output from Drop port, resulting in increased loss and crosstalk noise. When the resonance wavelength of MRs drifts to coincide with the working wavelength, most of the signals are coupled, which changes the direction of transmitted optical signal. In conclusion, MRs, as key components in ONoCs, are highly sensitive to thermal variations. Additional losses and crosstalk noise are introduced when the temperature on the ONoCs changes, which eventually lead to performance degradation or even functional failure of ONoCs.

III. Network Performance Analysis Based on Thermal Effect

Crosstalk noise and insertion loss are unavoidable problems in ONoCs, especially in large-size networks. They can seriously degrade network performance and even make ONoCs unable to communicate. Due to the thermo-optic effect, wavelength mismatch caused by temperature fluctuation introduces more crosstalk noise and loss. And these crosstalk and losses are dynamically changing with temperature. Therefore, the performance of ONoCs at different temperatures is different. In this section, we systematically analyze the network performance caused by thermal effect from the device level to the network level.

A. Quantitative Modeling of Basic Optical Elements

In ONoCs, basic optical switching elements are indispensable for the optical signals to be transmitted to the designated destination on a predetermined route. These optical elements are mainly composed of waveguides and MRs to transmit and change the original transmission direction of the optical signals. Three basic optical element structures including waveguide crossing, parallel switching elements (PSE) and crossing switching elements (CSE), as essential component in routers and networks, are systematically modeled and analyzed in this section. Fig. 3 illustrates the schematic diagram of three basic structures.

The waveguide crossing structure is shown in Fig. 3(e). The optical signal is input from the Input port and output from Out1 after through the intersection. At the intersection, a small part of the optical power is output from the Out2 and Out3 or reflect back to the Input port. This process causes the main optical signal to suffer a certain loss, and overflow part of the power becomes a potential interference signal in the ONoCs. The overflowed optical power is transmitted to other communication channels and becomes crosstalk noise. The output powers of each port are calculated through the following equations:

$$P_{O1} = L_c \cdot P_I \tag{21a}$$

$$P_{O2} = P_{O3} = C_c \cdot P_I \tag{21b}$$

$$P_r = C_r \cdot P_I \tag{21c}$$

where P_I is the input power of the optical signal and P_{Oi} is the output power of the port $Outi$. L_c and C_c represent the waveguide crossing loss coefficient and crosstalk noise coefficient, respectively.

The PSE in Fig. 3(a) and Fig. 3(b) consist of two parallel waveguides and a ring waveguide located therebetween. And the CSE in Fig. 3(c) and Fig. 3(d) are comprised of a waveguide crossing and a ring waveguide located in the vicinity thereof. Both of these switching elements include ON and OFF states. In the ON state, the wavelength of the input optical signal satisfies the resonance condition of the MRs. Most of the optical power is coupled into the MRs and output from the Drop port, which changes the direction of optical signal transmission. In the OFF state, the wavelength of the input optical signal does not satisfy the resonance condition of the MRs. Most of the optical signals travel forward along the original path without deflection. When the optical signal passes through these two types of switching elements, it also suffers a certain loss and generates some crosstalk noise. The output power of Through port and Drop port are represented by P_{T_p} and P_{D_p} when light signal passes through PSE, respectively. The following calculation models can

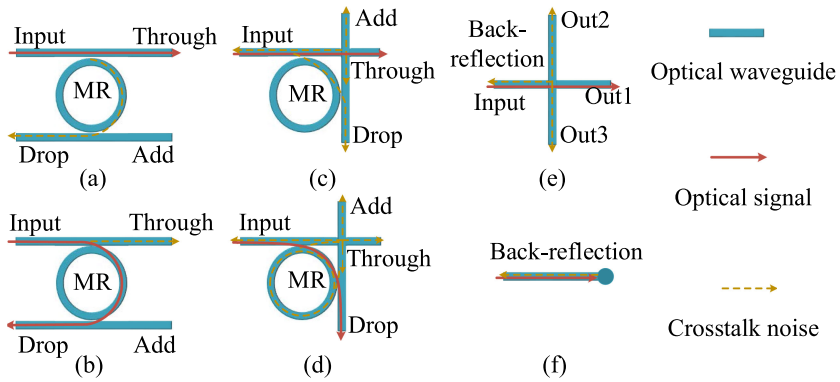

Fig. 3. (a) PSE in OFF state. (b) PSE in ON state. (c) CSE in OFF state. (d) CSE in ON state. (e) Waveguide crossing. (f) Optical terminator.

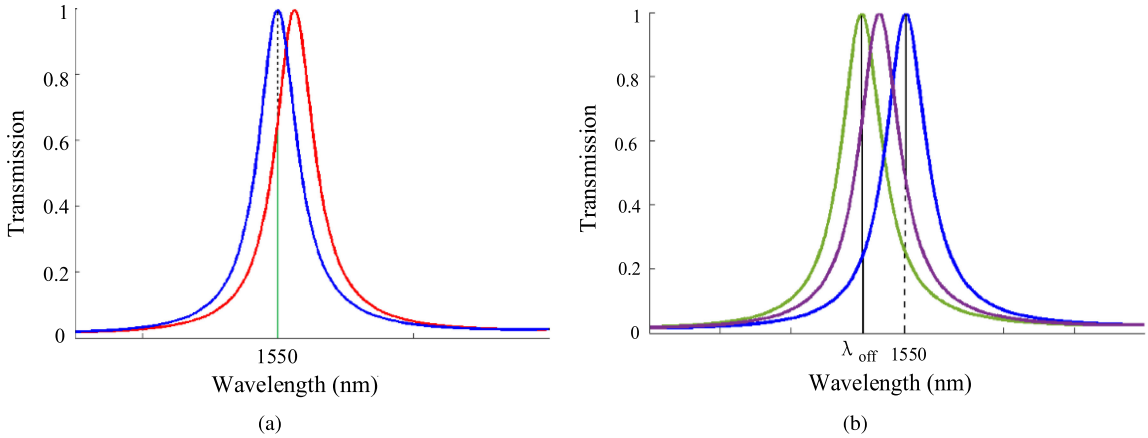

Fig. 4. MRs resonant wavelength drift diagram (a) in ON state and (b) in OFF state.

be obtained.

$$P_{T_p,on} = C_{p,on} \cdot P_I \tag{22a}$$

$$P_{D_p,on} = L_{p,on} \cdot P_I \tag{22b}$$

$$P_{T_p,off} = L_{p,off} \cdot P_I \tag{22c}$$

$$P_{D_p,off} = C_{p,off} \cdot P_I \tag{22d}$$

In the PSE, since the noise generated by the Add port is very small, so we do not consider it. In Eq. (22), $L_{p,on}$, $L_{p,off}$ and $C_{p,on}$, $C_{p,off}$ represent the loss coefficient and crosstalk coefficient of PSE in ON state and OFF state, respectively.

When the processor core runs at high speed, the temperature of the chip increases, which drives the resonant wavelength of the MRs on the chip to drift. This phenomenon results in the mismatch between the resonance wavelength of MRs and the working wavelength carrying information, which leads to the reduction of the transmittance of the working wavelength. Therefore, the loss coefficient and crosstalk coefficient all change dynamically with the fluctuation of temperature.

As shown in Fig. 4(a), the working wavelength and the initial resonance wavelength of MRs are 1550 nm, the MRs are in ON state, and the blue line is the initial transmission spectrum of MRs. With the change of temperature, the resonance wavelength of MRs changes, and its transmission is also changed, as shown in the red spectrum. At this time, the transmittance of the working wavelength decreases (green solid line), which means the loss coefficient $L_{p,on}$ decreases, and the overflow crosstalk noise $C_{p,on}$ increases (green dotted line). According to the theoretical analysis of MRs, the relationship between $L_{p,on}$ and temperature T can be expressed as follows:

$$\begin{aligned} L_{p,on} = {} & a_1 \cdot exp\left(-\left(\frac{\lambda_w - \mu T + \mu T_0 - b_1}{c_1}\right)^2\right) \\ & + a_2 \cdot exp\left(-\left(\frac{\lambda_w - \mu T + \mu T_0 - b_2}{c_2}\right)^2\right) \\ & + a_3 \cdot exp\left(-\left(\frac{\lambda_w - \mu T + \mu T_0 - b_3}{c_3}\right)^2\right) \\ & + a_4 \cdot exp\left(-\left(\frac{\lambda_w - \mu T + \mu T_0 - b_4}{c_4}\right)^2\right) \\ & + a_5 \cdot exp\left(-\left(\frac{\lambda_w - \mu T + \mu T_0 - b_5}{c_5}\right)^2\right) \end{aligned} \tag{23}$$

where the λ_w is working wavelength. The corresponding crosstalk coefficient $C_{p,on}$ in ON state can be expressed as:

$$C_{p,on} = L_{p,on_{top}} + C_{p,on_{min}} - L_{p,on} \tag{24}$$

Here we do not use $1 - L_{p,on}$ to indicate the crosstalk coefficient because we consider the loss caused by the transmission process and a small part of the optical power spilled from the Add port. The values of $L_{p,on_{top}}$ and $C_{p,on_{min}}$ are -0.5 dB and -25 dB, respectively [21].

For PSE in OFF state, the loss coefficient $L_{p,off}$ and crosstalk coefficient $C_{p,off}$ also vary with temperature fluctuation, and they are closely related to the resonance wavelength λ_{off} of MRs in OFF state. If λ_{off} falls to the right of the working wavelength (1550 nm), the loss and crosstalk noise do not increase due to thermal wavelengths deviated. If λ_{off} falls to the left of 1550 nm, the loss and crosstalk coefficients increase with the thermal drift of MRs resonant wavelength. As shown in Fig. 4(b), the green spectral line is the transmission spectrum of MRs in OFF state. With the fluctuation of temperature, the transmission spectrum of MRs drifts to the position of purple line or blue line, and the transmittance of 1550 nm changes (dotted line), so the values of $L_{p,off}$ and $C_{p,off}$ also change. The expression of $L_{p,off}$ can be expressed as follows:

$$\begin{aligned} L_{p,off} &= L_{p,on_{top}} + C_{p,on_{min}} \\ &- \left(a_1 \cdot exp\left(- \left(\frac{(\lambda_w - \Delta\lambda) + (1550 - \lambda_{off}) - b_1}{c_1} \right)^2 \right) \right. \\ &+ a_2 \cdot exp\left(- \left(\frac{\lambda_w - \Delta\lambda) + (1550 - \lambda_{off}) - b_2}{c_2} \right)^2 \right) \\ &+ a_3 \cdot exp\left(- \left(\frac{\lambda_w - \Delta\lambda) + (1550 - \lambda_{off}) - b_3}{c_3} \right)^2 \right) \\ &+ a_4 \cdot exp\left(- \left(\frac{\lambda_w - \Delta\lambda) + (1550 - \lambda_{off}) - b_4}{c_4} \right)^2 \right) \\ &+ \left. a_5 \cdot exp\left(- \left(\frac{\lambda_w - \Delta\lambda) + (1550 - \lambda_{off}) - b_5}{c_5} \right)^2 \right) \right) \end{aligned} \tag{25a}$$

$$\Delta\lambda = \mu(T - T_0) \tag{25b}$$

The corresponding crosstalk coefficient $C_{p,on}$ in ON state can be expressed as:

$$C_{p,off} = L_{p,off_{top}} + C_{p,off_{min}} - L_{p,off} \tag{26}$$

The values of $L_{p,off_{top}}$ and $C_{p,off_{min}}$ are -0.005 dB and -20 dB, respectively [20]. In PSE, the negligible crosstalk noise of Add port is not considered.

Compared with the PSE, CSE can be regarded as a combination of PSE and waveguide crossing, so the loss and crosstalk noise of waveguide crossing are inevitably introduced. Accordingly, the power model of the CSE in two states can be obtained by the power model of the PSE and the waveguide crossing in two states. The output power of each port of the CSE in ON state shown in Fig. 3(c) can be expressed by the following formula.

$$P_{T_c,on} = C_{p,on} \cdot P_I \cdot (L_c(1 + C_c \cdot L_{p,on}) + C_r \cdot L_{p,on} \cdot C_c) \tag{27a}$$

$$P_{D_c,on} = L_{c,on} \cdot P_I \tag{27b}$$

$$P_{A_c,on} = C_{p,on} \cdot P_I \cdot (C_c(1 + C_c \cdot L_{p,on}) + C_r \cdot L_{p,on} \cdot L_c) \tag{27c}$$

$$P_{R_c,on} = C_{p,on} \cdot C_r \cdot P_I \tag{27d}$$

Parameter $L_{c,on} = L_{p,on} + {C_{p,on}}^2 \cdot C_c$ is the loss coefficient of CSE in ON state, which can be calculated from the models of PSE and the waveguide crossing. The CSE in OFF state is shown in Fig. 3(d). The output power of each port can be expressed as:

$$P_{T_c,off} = L_{c,off} \cdot P_I \tag{28a}$$

$$P_{D_c,off} = (C_{p,off} + {L_{p,off}}^2 \cdot C_c) \cdot P_I \tag{28b}$$

$$P_{A_c,off} = C_c \cdot L_{p,off} \cdot P_I \tag{28c}$$

$$P_{R_c,off} = C_r \cdot {L_{p,off}}^2 \cdot P_I \tag{28d}$$

The $L_{c,off}$ is the loss coefficient of CSE in OFF state, and it can be expressed as: $L_{c,off} = L_c \cdot L_{p,off}$. The reflected power P_{Tr} of the optical terminator can be written as $P_{Tr} = C_t \cdot P_I$.

B. Quantitative Modeling of Mesh-Based ONoCs

Based on the proposed thermal effect power models of basic optical elements, we systematically analyze the models for mesh-based ONoCs in network levels. The theoretical models of loss, crosstalk noise and OSNR caused by thermal effect at network level are established, and the worst SNR link is found for ONoCs performance analysis. The worst SNR link needs to satisfy two conditions: (1) The link should have a high power loss. (2) The link suffers from higher crosstalk noise from other links.

A $M \times N$ mesh-based ONoCs is composed of $M \times N$ processing cores, $M \times N$ five-port routers and several waveguides connected according to mesh topology, as shown in Fig. 5(a). As the heart of ONoCs, the performance of router directly affects the communication quality of the whole ONoCs communication system. And the router contains many MRs, so the influence of temperature fluctuation on the chip is absolutely not negligible. In order to detailedly analyze the effects of thermal effect on the performance of ONoCs, the performance analysis of routers based on thermal effect is an indispensable part. Fig. 5(b) shows a general 5×5 optical router model used in mesh-based ONoCs, which is based on dimension-order routing algorithm. The router has five bidirectional ports represented by I_k^h, and its Injection/Ejection, North, East, South, and West ports represented by subscripts $0, 1, 2, 3, 4$ clockwise. The superscript h represents the input and output state of the port, 0 denotes input port and the 1 denotes output port.

When an optical signal is transmitted from port m to port n of router $R(x, y)$, the output optical power $P_{m,n}^R(x, y)$ can be obtained by Eq. (29).

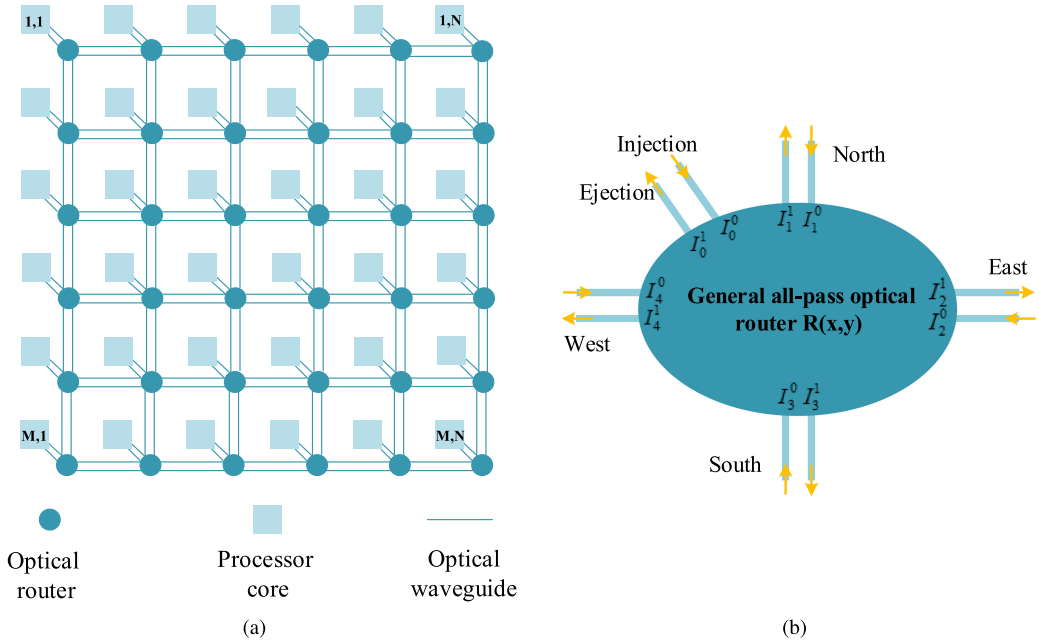

Fig. 5. (a) $M \times N$ mesh-based ONoCs. (b) General 5×5 optical router model.

$$P^R_{m,n}(x,y) = P^R_I(x,y) \cdot L^R_{m,n}(x,y) \tag{29a}$$

$$L^R_{m,n}(x,y) = L^R_{E_{m,n}}(x,y) \cdot L_b \cdot L_p \tag{29b}$$

$$m,n \in (0,...,4), x \in (1,...,M), y \in (1,...,N)$$

where the $P^R_I(x,y)$ and the $L^R_{m,n}(x,y)$ are input optical power of router $R(x,y)$ and the insertion loss of the optical signal transmitted from the port m to the port n of the $R(x,y)$, respectively. And the $L^R_{m,n}(x,y)$ includes loss $L^R_{E_{m,n}}(x,y)$ caused by basic optical elements, waveguide bending loss L_b and propagation loss L_p in optical router $R(x,y)$. The L_p is a function of optical signal transmission length L and the waveguide attenuation coefficient α.

$$L_p = 10^{-\alpha L/10} \tag{30}$$

When the main signal is transmitted from port m to port n of router $R(x,y)$, if the other idle port pairs transmit another optical signal at the same time and there is a path intersection with the main signal, the crosstalk noise will accumulate on the main signal. $P^R_{N_{m,n}}(x,y)$ is defined as the crosstalk noise power accumulated on the main signal traveling from the port m to the port n of the router $R(x,y)$.

$$P^R_{N_{m,n}}(x,y) = \sum_{i=0}^{4}(P_{I(i)}(x,y) \cdot C_{m,n,i}(x,y)) \tag{31}$$

$$m,n \in (0,...,4), x \in (1,...,M), y \in (1,...,N)$$

In Eq. (31), the i is the idle port that introduces crosstalk noise, $C_{m,n,i}(x,y)$ is the crosstalk coefficient of the transmission link, and $P_{I(i)}(x,y)$ is the input optical signal power of port i.

In mesh-based ONoCs, we have to make several assumptions in order to make it possible to analyze its network performance. Firstly, we assume that the signal suffers the same loss when transmitted in the same input and output ports in different routers. Therefore, the above $L^R_{m,n}(x,y)$ are represented by $L^R_{m,n}$, as in Eq. (32a). Secondly, as shown in Eq. (32b), the value of $C_{m,n,i}$ multiplied by another crosstalk coefficient is very small and can be ignored. Finally, it is assumed that the input optical power at Injection ports of the optical router at different locations is the same as shown in Eq. (32c).

$$L^R_{m,n}(x_0,y_0) = L^R_{m,n}(x_1,y_1) = L^R_{m,n} \tag{32a}$$

$$C_{m_0,n_0,i_0} \cdot C_{m_1,n_1,i_1} \approx 0,$$

$$m_0,n_0,i_0,m_1,n_0,i_1 \in (0,...,4) \tag{32b}$$

$$P^R_I(x_0,y_0) = P^R_I(x_1,y_1) = P^R_I \tag{32c}$$

The information transmission in Mesh-based ONoCs follows the dimension-order routing algorithm, that is, the optical signal from the source node to the destination node must first be transmitted in the X direction and then in the Y direction. During transmission, optical signals suffer a certain loss when passing through routers and waveguides in the network. Therefore, the output optical power when the optical signal is transmitted from the source node (x_0,y_0) to the destination node (x_1,y_1) can be expressed as follows:

$$P_{(x_0,y_0),(x_1,y_1)} = P^R_I \cdot L_{(x_0,y_0),(x_1,y_1)} \cdot L_{p_D} \tag{33a}$$

$$L_{p_D} = 10^{-\frac{\alpha \cdot ((x_1-x_0)\cdot L_x + (y_1-y_0)\cdot L_y)}{10}} \tag{33b}$$

The $L_{(x_0,y_0),(x_1,y_1)}$ and L_{p_D} represent the loss caused by the router and the transmission loss caused by the optical waveguide between routers, respectively. And L_x and L_y represent the waveguide distances between adjacent two routers in the x-axis direction and the y-axis direction, respectively. d is used

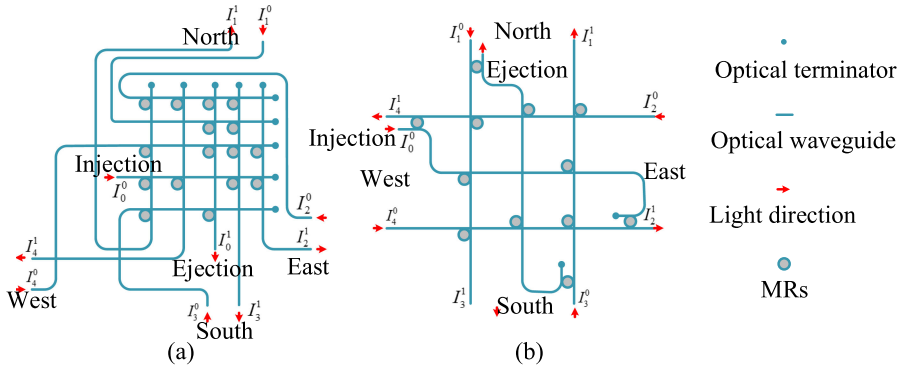

Fig. 6. (a) Crossbar router. (b) Crux router.

to indicate the diameter of Si wafers, there are the following equations:

$$((M-1)\cdot L_y)^2 + ((N-1)\cdot L_x)^2 = d^2 \tag{34}$$

According to the symmetry and uniformity of the mesh-based ONoCs, we can assume that $M = N$ and $L_x = L_y$.

$$L_x = L_y = \frac{\sqrt{2}}{2}\cdot\frac{d}{M-1} = \frac{\sqrt{2}}{2}\cdot\frac{d}{N-1} \tag{35}$$

Based on the above analysis and references [4], [6], the crosstalk noise power accumulated in the destination node is as follows:

$$P_{N(x_0,y_0),(x_1,y_1)} = \sum_{(x_0,y_0)}^{(x_1,y_1)} \frac{P_{N(x_i,y_i)}\cdot L_(x_0,y_0),(x_1,y_1)}{L_(x_0,y_0),(x_i,y_i)} \tag{36}$$

which is formed by superimposing the noise accumulated in each router of the communication link after loss to the destination node. In Eq. (36), $P_{N(x_i,y_i)}$ is the crosstalk noise power assembled in the optical router $R(x_i, y_i)$ of the communication link.

The optical signal-to-noise ratio (OSNR) and bit error rate (BER) can be calculated as important parameters to evaluate the performance of ONoCs, which are expressed as:

$$OSNR = 10log\left(\frac{P_{(x_0,y_0),(x_1,y_1)}}{P_{N(x_0,y_0),(x_1,y_1)}}\right) \tag{37}$$

$$BER = \frac{1}{2}\left(1 - \frac{2}{\sqrt{\pi}}\int_0^{\frac{\sqrt{OSNR}}{2}} e^{-t^2}dt\right) \tag{38}$$

IV. Numerical Simulation and Result Analysis

We take a numerical simulation on the worst SNR links of mesh-based ONoCs using different routers at different temperatures based on the analytical model mentioned above, and systematically analyze the performance of mesh-based ONoCs based on thermal effect. The numerical simulation is based on the MATLAB environment. And the two optical routers used are crossbar router and crux router as shown in Fig. 6, they all conform to the general optical router model previously analyzed.

TABLE I
Loss, Crosstalk, and Reflectance Coefficients

Parameter	Value	Reference
L_c	-0.04 dB	[22]
L_p	-0.274 dB/cm	[23]
L_b	-0.005 dB/90°	[24]
C_c	-40 dB	[22]
C_r	≅ 0	[22]
C_t	-50 dB	[25]

In addition, in the simulation example, the Si wafer used is 4 inches [26], the input power is 0 dBm and the other parameters used are shown in Table I.

From the analysis in the second section, the worst OSNR link has the highest loss and the largest crosstalk noise. Although the longest link contains the most routers and has the highest loss, it does not necessarily have the highest crosstalk. Based on these factors, we simulate the different directions of the first, second and third long links, and find the worst SNR links based on mesh-based ONoCs. As shown in Fig. 7, the worst SNR links for mesh-based ONoCs using crossbar and crux router are the first longest link from the processor core (1, N) to the processor core (M, 1) and the second longest link from processor core (M, 1) toward the core (1, N-1) respectively when the temperature changes. The red line in the Fig. 7 represents the path of optical signal transmission in the worst SNR link, and the yellow dotted line is the path in which crosstalk noise is introduced.

Fig. 8(a) and 8(b) show the power for the received optical signal and crosstalk noise of the destination node in mesh-based ONoCs using crux router and crossbar router at different temperatures, respectively. The X and Y axes correspond to the network scale M and N, and the Z axes represent the values of signal power and crosstalk noise power. Fig. 8 shows that in two networks with different routers, the power of optical signals received by the target node drops rapidly while the power of crosstalk noise increases relatively slowly with the increase of network size. However, when the temperature rises, the speed of

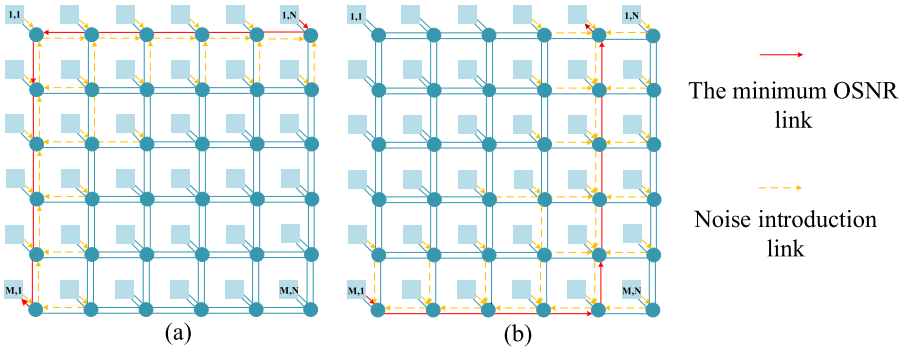

Fig. 7. The worst SNR links in mesh-based ONoCs using (a) crossbar router and (b) crux router.

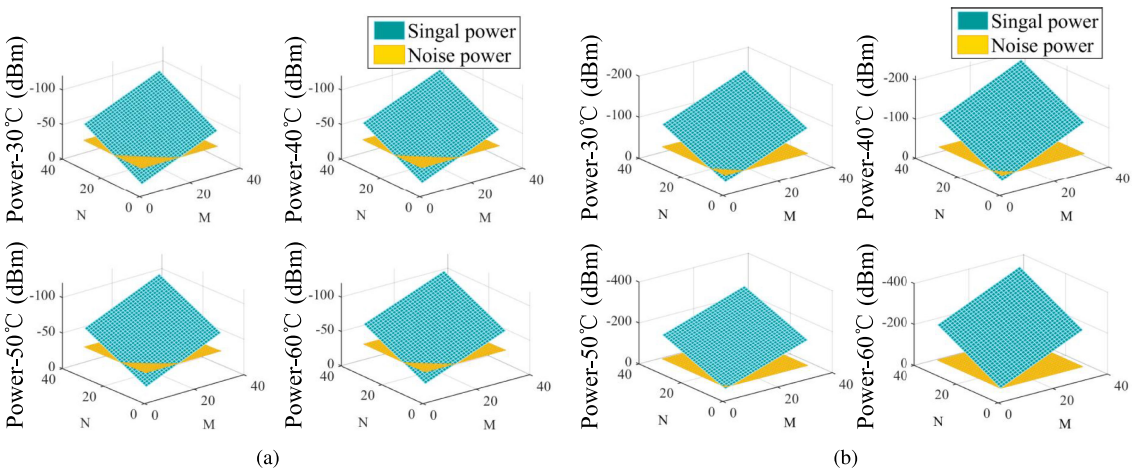

Fig. 8. Signal power and crosstalk noise power comparison in $M \times N$ mesh-based ONoCs using two routers. (a) crux router. (b) crossbar router.

the signal power drops and crosstalk noise power increases are accelerated significantly. Of course, compared with mesh-based ONoCs using crux router, the decrease of signal power and the increase of crosstalk noise power are more obvious in ONoCs using crossbar router. This is because the crossbar router has a large insertion loss, which not only reduces the optical signal power but also the crosstalk noise power in the signal transmission process.

Using the network performance analysis model based on thermal effect proposed in this paper, the variation of OSNR of the worst SNR link in mesh-based ONoCs with temperature and network size can be obtained. Fig. 9(a) depicts the OSNR of the mesh-based ONoCs using the crux router, Fig. 9(b) illustrates the OSNR of the mesh-based ONoCs using the crossbar router. The X axis and Y axis are, respectively, the network size and temperature of ONoCs, and the Z axis is the corresponding OSNR value. Fig. 9 shows that networks using crux router have better OSNR performance than networks using crossbar router at the same network size. In addition, with the expansion of network size and the increase of temperature, the OSNR of the worst SNR link in the mesh-based ONoCs using both routers have a downward trend. When the network scale is small, the influence of temperature on network OSNR performance is weaker than network size. When the network size increases to a certain extent, the OSNR for the worst SNR link of mesh-based ONoCs decreases sharply with the increase of temperature. Compared with mesh-based ONoCs using crux router, this phenomenon is more obvious in mesh-based ONoCs using crossbar router. This is because crossbar routers have more MRs than curx router. With the enlargement of network size, the number of MRs in the ONoCs increases dramatically, and the loss and crosstalk noise caused by fluctuation of temperature also increase sharply.

Moreover, the maximum network size of mesh-based ONoCs can be obtained by using the criterion that the optical power output by the destination node of the worst OSNR link is approximately equal to the crosstalk noise power accumulated at that node. In other words, the OSNR of the worst SNR link is close to zero. When the network scale is larger than the maximum network size, the network drop its communication function. The simulation results show that the maximum network size of mesh-based ONoCs using crux router is 11×11 when the temperature is 30 °C. As the temperature rises, the maximum network size gradually shrinks. When the temperature rises to 60 °C, it decreases to 9×9. However, the maximum network size of mesh-based ONoCs using crossbar router at 30 °C is 7×7, and when the temperature is 60 °C, it shrinks to 3×3.

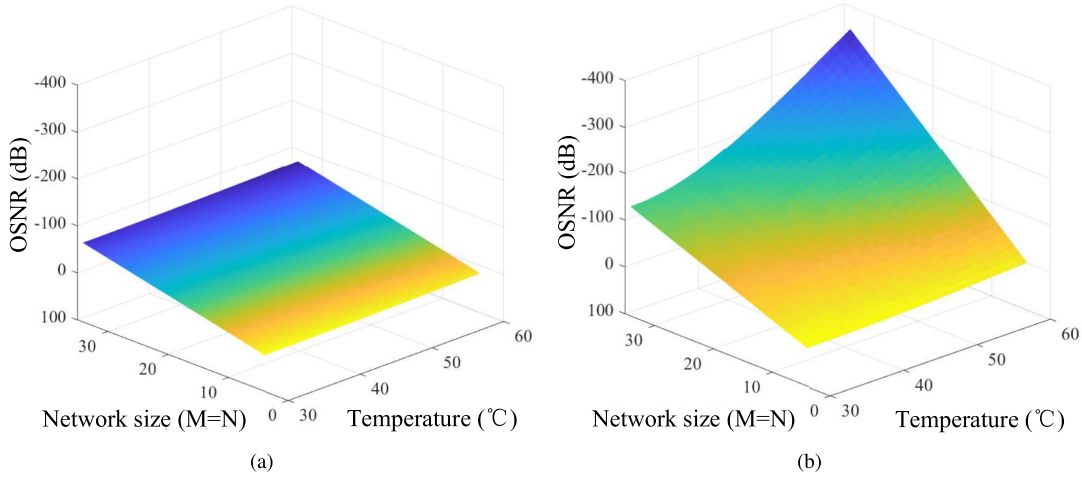

Fig. 9. Variation of OSNR of the worst SNR link in mesh-based ONoCs with temperature and network size. (a) crux router. (b) crossbar router.

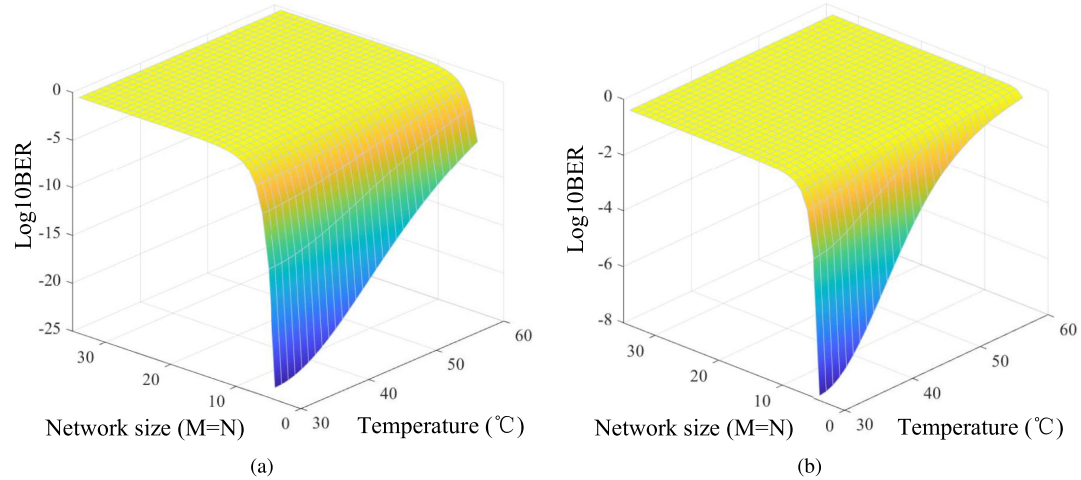

Fig. 10. Maximum BER of mesh-based ONoCs based on thermal effect. (a) crux router. (b) crossbar router.

Obviously, this is the scalability reduction of network scale caused by the introduction of more loss and crosstalk noise by the MRs included in the router with the change of temperature.

Similarly, using the proposed network performance analysis model, we can get the maximum BER of mesh-based ONoCs based on thermal effect. Fig. 10(a) and Fig. 10(b) show the maximum BER of mesh-based ONoCs using crux router and crossbar router, respectively. According to the Fig. 10, it can be clearly observed that mesh-based ONoCs using crossbar router have a higher BER than using crux router, and the BER of both networks change with the expansion of network size and the fluctuate of temperature. The change trend of BER with the increase of network size is that it gradually increases and eventually tends to a relatively stable value, while the trend of change with temperature is relatively gentle than that with network size. And when the network size is small, the trend of BER with temperature is similar to an S-curve.

In order to further explore the influence of temperature fluctuation on the transmission characteristics of optical signals, we built mesh-based ONoCs communication transmission systems using two routers in the optisystem simulation environment based on the data obtained from the MATLAB simulation environment. As shown in Fig. 11, the system consists of signal module S(t), noise module N(t) and transmission system. In S(t), we use pseudo random bit sequence (PRBS) generator to generate pseudo random sequence with bit rate of 10 Gb/s to simulate the information source in communication. In addition, we choose a CW laser with 1 mW power and 1550 nm wavelength as the light source to modulate the signals. In the N(t), the multi-channel crosstalk noise in the system is simulated by combining multiple optical signals with different time delays. Then noise and signal are transmitted simultaneously in the transmission system. Finally, the transmitted optical signal is converted into electrical signal by a photodetector.

Fig. 12 shows the eye diagrams of 6×6 mesh-based ONoCs using crux router and crossbar router at different temperatures. The eye diagrams can intuitively demonstrate the communication quality of networks. It can be seen from the Fig. 12 that

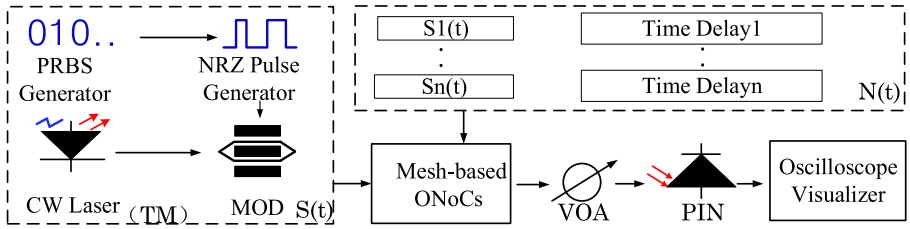

Fig. 11. Diagram of the simulation setup used for simulating the performance of mesh-based ONoCs.

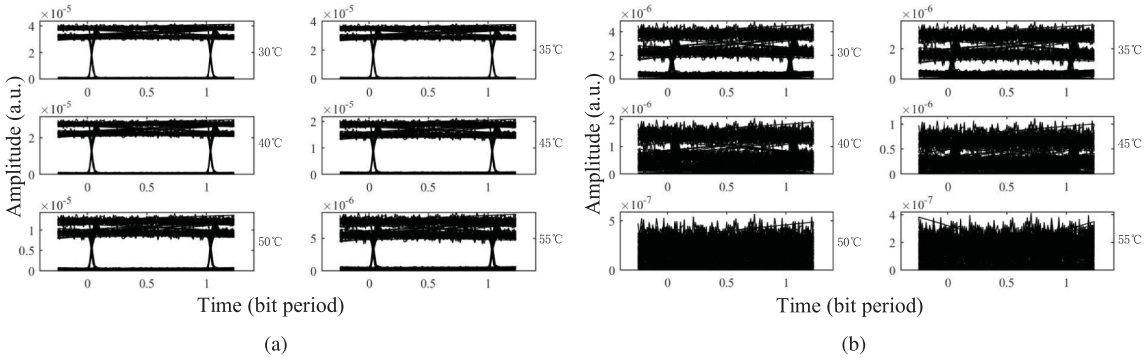

Fig. 12. Eye diagrams of 6 × 6 mesh-based ONoCs at different temperatures using (a) crux router and (b) crossbar router.

with the increase of temperature, the quality of eye diagrams decreases gradually, which is more obvious in the ONoCs using crossbar router than in the ONoCs using crux router. This phenomenon is due to the continuous introduction of additional crosstalk noise power with the increase of temperature. The greater temperature changes, the more thermal crosstalk noise and loss will be introduced. Moreover, there are more MRs in crossbar router than in crux router, so there are more thermal noise and crosstalk introduced. This is consistent with our simulation results above.

V. Conclusion

During the running of ONoCs, the temperature on the chip can fluctuate temporally as well as spatially. This phenomenon brings extra loss and crosstalk noise to network, which makes the network performance decline sharply. In order to propose a better solution to this problem, it is very important to analyze the influence of thermal effect in ONoCs network. In this paper, a network performance analysis model of thermal effect in mesh-based ONoCs is proposed for the first time. Specific functional relationships between temperature and loss, crosstalk noise are established. And performance analysis criteria of thermal effect are proposed from basic optical elements level to network level. Moreover, based on the simulation environment of MATLAB, we have established a numerical simulation system to evaluate the proposed model and found the worst SNR link in the mesh-based ONoCs. Finally, we employ the system to simulate the network performance of thermal effect in mesh-based ONoCs using crossbar and crux router. The signal power, crosstalk noise power, OSNR and BER of the worst SNR link destination node in mesh-based ONoCs are analyzed. The simulation results show that the network performance of mesh-based ONoCs decreases with the increase of temperature regardless of which router is used. This indicates that the temperature fluctuation on the chip can greatly affect the network performance of ONoCs. The proposed ONoCs network performance analysis model of thermal effect not only provides analysis criteria for network performance analysis of ONoCs based on thermal effect, but also provides technical support for future research of ONoCs.

References

[1] A. Shacham, K. Bergman, and L. P. Carloni, "Photonic networks-on-chip for future generations of chip multiprocessors," *IEEE Trans. Comput.*, vol. 57, no. 9, pp. 1246–1260, Sep. 2008.

[2] R. Beausoleil, P. Kuekes, G. Snider, S.-Y. Wang, and R. Williams, "Nanoelectronic and nanophotonic interconnect," *Proc. IEEE*, vol. 96, no. 2, pp. 230–247, Feb. 2008.

[3] K. Skadron, M. R. Stan, K. Sankaranarayanan, W. Huang, S. Velusamy, and D. Tarjan, "Temperature-aware microarchitecture: Modeling and implementation," *ACM Trans. Arch. Code Optim.*, vol. 1, no. 1, pp. 94–125, Mar. 2004.

[4] Y. Xie, W. Xu, W. Zhao, Y. Huang, T. Song, and M. Guo, "Performance optimization and evaluation for torus-based optical networks-on-chip," *J. Lightw. Technol.*, vol. 33, no. 18, pp. 3858–3865, Sep. 2015.

[5] Y. Xie *et al.*, "Formal worst-case analysis of crosstalk noise in mesh-based optical networks-on-chip," *IEEE Trans. Very Large Scale Integr. Syst.*, vol. 21, no. 10, pp. 1823–1836, Oct. 2013.

[6] Y. Xie, T. Song, Z. Zhang, C. He, J. Li, and C. Xu, "Formal analysis of crosstalk noise in mesh-based optical networks-on-chip with WDM," *J. Lightw. Technol.*, vol. 34, no. 15, pp. 3550–3562, Aug. 2016.

[7] J. Zhang and Y. Xie, "Exploiting worst-case OSNR in fat-tree-based optical networks-on-chip employing WDM," in *Proc. IEEE Int. Conf. 3M-NANO*, 2017, pp. 278–283.

[8] R. Amatya *et al.*, "Low power thermal tuning of second-order microring resonators," in *Proc. Conf. Lasers Electro-Opt.*, 2007, pp. 6–11.

[9] M. Meyer, Y. Okuyama, and A. B. Abdallah, "SAFT-PHENIC: A thermal-aware microring fault-resilient photonic NoC," *J. Supercomput.*, vol. 74, no. 9, pp. 4672–4695, Sep. 2018.

[10] H. Li, A. Fourmigue, S. Le Beux, X. Letartre, I. O'Connor, and G. Nicolescu, "Thermal aware design method for VCSEL-based on-chip optical interconnect," in *Proc. IEEE Des., Automat. & Test Europe Conf. & Exhib.*, 2015, pp. 1120–1125.

[11] W. Bogaerts *et al.*, "Silicon microring resonators," *Laser Photon. Rev.*, vol. 6, no. 1, pp. 47–73, 2012.

[12] Y. Vlasov and S. McNab, "Losses in single-mode silicon-on-insulator strip waveguides and bends," *Opt. Exp.*, vol. 12, no. 8, pp. 1622–1631, Apr. 2004.

[13] S. Xiao, M. H. Khan, H. Shen, and M. Qi, "Modeling and measurement of losses in silicon-on-insulator resonators and bends," *Opt. Exp.*, vol. 15, no. 17, pp. 10553–10561, Aug. 2007.

[14] W. Liu, P. Wang, M. Li, Y. Xie, and N. Guan, "Quantitative modeling of thermo-optic effects in optical networks-on-chip," in *Proc. ACM Great Lakes Symp. VLSI*, 2017, pp. 263–268.

[15] Y. Ye *et al.*, "System-level modeling and analysis of thermal effects in optical networks-on-chip," *IEEE Trans. Very Large Scale Integr. Syst.*, vol. 21, no. 2, pp. 292–305, Feb. 2013.

[16] Y. Ye *et al.*, "System-level modeling and analysis of thermal effects in WDM-based optical networks-on-chip," *IEEE Trans. Comput-Aided Des. Integr. Circuits Syst.*, vol. 33, no. 11, pp. 1718–1731, Nov. 2014.

[17] M. Li, W. Liu, L. Yang, Y. Xie, Y. Ye, and N. Guan, "Work-in-progress: Communication optimization for thermal reliable many-core systems," in *Proc. Int. Conf. Hardware/Software Codesign Syst. Synthesis*, 2017, pp. 1–2.

[18] Z. Li, M. Mohamed, X. Chen, E. Dudley, K. Meng, and L. Shang, "Reliability modeling and management of nanophotonic on-chip networks," *IEEE Trans. Very Large Scale Integr. Syst.*, vol. 20, no. 1, pp. 98–111, Jan. 2012.

[19] F. G. Della Corte, M. E. Montefusco, L. Moretti, I. Rendina, and G. Cocorullo, "Temperature dependence analysis of the thermo-optic effect in silicon by single and double oscillator models," *J. Appl. Phys.*, vol. 88, no. 12, pp. 7115–7119, Dec. 2000.

[20] J. Komma, C. Schwarz, G. Hofmann, D. Heinert, and R. Nawrodt, "Thermo-optic coefficient of silicon at 1550 nm and cryogenic temperatures," *Appl. Phys. Lett.*, vol. 101, no. 4, pp. 1905-1–1905-4, Jul. 2012.

[21] J. Chan, G. Hendry, K. Bergman, and L. Carloni, "Physical-layer modeling and system-level design of chip-scale photonic interconnection networks," *IEEE Trans. Comput.-Aided Des. Integr. Circuits Syst.*, vol. 30, no. 10, pp. 1507–1520, Oct. 2011.

[22] W. Ding, D. Tang, Y. Liu, L. Chen, and X. Sun, "Compact and low crosstalk waveguide crossing using impedance matched metamaterial," *Appl. Phys. Lett.*, vol. 96, no. 11, pp. 111114–111116, Mar. 2010.

[23] P. Dong *et al.*, "Low loss silicon waveguides for application of optical interconnects," in *Proc. IEEE Photon. Soc. Summer Topical Meeting Ser.*, 2010, pp. 191–192.

[24] F. Xia, L. Sekaric, and Y. Vlasov, "Ultracompact optical buffers on a silicon chip," *Nature Photon.*, vol. 1, pp. 65–71, Dec. 2007.

[25] G. R. Zhou, X. Li, and N. N. Feng, "Design of deeply etched antireflective waveguide terminators," *IEEE J. Quantum Electron.*, vol. 39, no. 2, pp. 384–391, Feb. 2003.

[26] S. H. Kim *et al.*, "High performance InGaAs-on-insulator MOSFETs on Si by novel direct wafer bonding technology applicable to large wafer size Si," in *Proc. Symp. VLSI Technol.*, 2014, pp. 1–2.